International Journal of Environmental Sciences
ISSN: 2229-7359
Vol. 11 No. 3s,2025
https://theaspd.com/index.php

Segmentation Of Medical Images Using Deep Learning

Priyanka Gupta[1], Aakansha Soy[2], Rachna Kathuria[3]
[1]Assistant Professor, Department of Chemistry, Kalinga University, Raipur, India.
[2]Assistant Professor, Department of CS & IT, Kalinga University, Raipur, India.
ku.aakanshasoy@kalingauniversity.ac.in, 0009-0002-1955-6909
[3]Assistant Professor, New Delhi Institute of Management, New Delhi, India., E-mail: rachna.kathuria@ndimdelhi.org, https://orcid.org/0000-0002-7773-0269

Abstract
It offers computerized delineation of particular anatomical structures of interest and also facilitates numerous subsequent tasks like shape analysis and volume measurement. Specifically, the fast innovation of deep learning methods in the past few years has significantly contributed to improving the performance of segmentation algorithms by making effective use of large amounts of labelled data in order to improve complex models. Nevertheless, obtaining manual labels to train can become a significant burden for the applicability of learning-based approaches in medical images. Scientists have investigated numerous unsupervised and semi-supervised learning techniques to lessen the labelling limitation in an effort to address this problem. This chapter presents the fundamental ideas of deep learning-based segmentation as well as some of the most advanced techniques now in use, arranged according to the level of supervision. Our aim is to give the reader some potential solutions for model choice, training strategy, and data manipulation based on a certain segmentation task and dataset.
Keywords: *Image segmentation, Deep learning, Medical images*

I INTRODUCTION

Since a number of improvements in biomedical image acquisition systems over the years has led to increased usage frequency of modalities in the non-invasive exercise of disease diagnosis [10]. Computed tomography (CT) increased by 7.8%, magnetic resonance imaging (MRI) by 10%, and positron emission tomography (PET) by 57% in the United States between 1996 and 2010, indicating a major change in medical imaging techniques.[1] Examined trends and patterns from 2004-2014 relating to applications of biomedical imaging in Brazil's public healthcare system, wherein observable increase in their use was evident, particularly that of CT and MRI, with 12% and 19% yearly increments respectively [2]. Though the number of biomedical images that are routinely acquired is on the rise, such increasing behaviour is not observed for the number of experts or specialists who analyses or examines such scans [9]. Most of the healthcare applications require critical examination of biomedical imaging for diagnosis and follow-up treatment plans [15]. However, manual analysis of such scans is tedious, slow, expensive and prone to error. This disparity in quality of care and diagnosis demands an automated biomedical image analysis system that could lower the burden on experts along with the faster diagnosis and treatment of the diseases [8]. With the growing use of electronic health records (EHRs), deep learning algorithms have become more and more important in the healthcare industry, allowing for better patient care, enhanced data analysis, and pattern identification [3][12]. Over the past decades, there are massive advancements in deep learning technologies for computer vision problems involving object detection, classification, localization, segmentation, etc[4]. Following such advancements in deep learning along with the wide availability of publicly accessible biomedical imaging data information in terms of microscopy imaging (e.g., bright-field, fluorescence or electron microscopy), MRI, X-ray, CT, PET, ultrasound (US), etc., there is a significant gain in the momentum of its applications in biomedical image analysis [13].

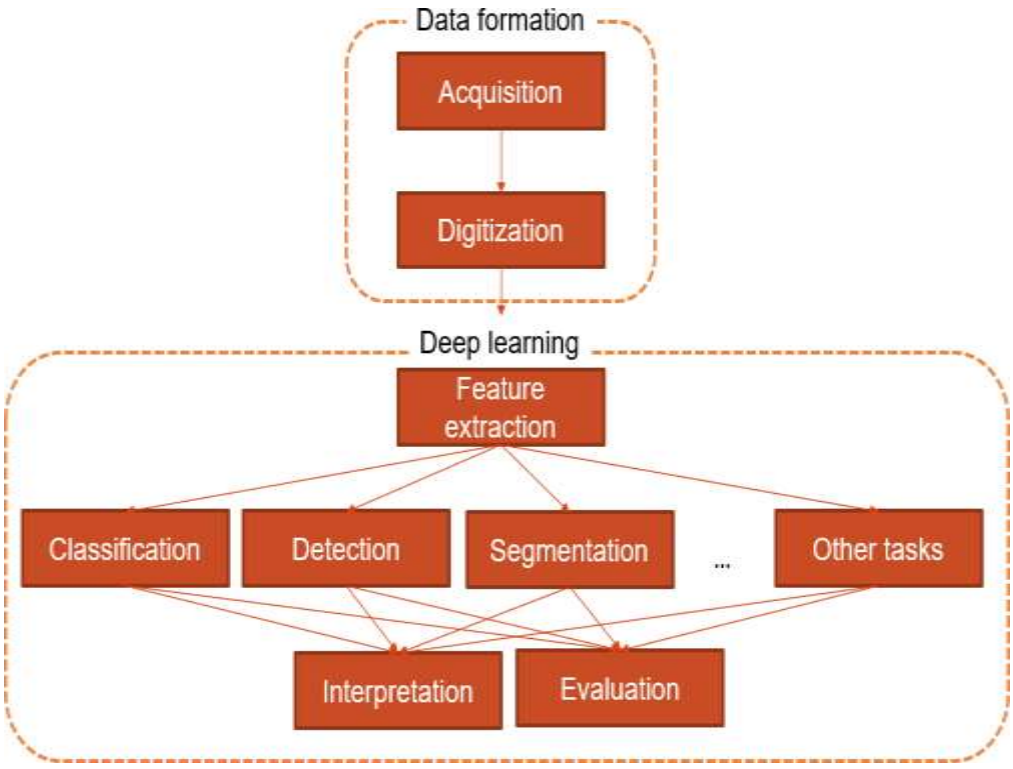

Figure 1. Overview of the steps involved in any deep learning based biomedical image analysis system.

The success of deep learning in image analysis has inspired biomedical imaging researchers to explore its possibilities in analyzing a number of medical modalities to help clinicians in quicker diagnosis and treatment of disease or infection. [5] [11] Any deep learning based biomedical image analysis system can be divided into data formation phase and deep learning phase as shown in Fig.1. Initially, in the data formation phase data is collected via various medical image acquisition systems, followed by image enhancement strategies such as calibration, filtering, transformations, etc. and later, digitized for analysis [7,8]. This phase is generally performed by experts to make data accessible for diagnosis and treatment. Later, the generated dataset can be utilized by the biomedical image research community to perform quantitative measurements and abstract interpretations of biomedical images by performing classification, detection, segmentation, localization, etc., using CNN models [6]. The performance of the trained models is assessed, and interpretations are produced to confirm their resilience, guaranteeing the precision and dependability of the forecasts.

III METHODOLOGY

There are 10.5 million trainable parameters in the architectural design, which includes elements such as multi-modality fusion, segmenter, and tumor extractor. The tumor extractor combines pre-processed multi-modalities to extract features using down-sampling and max-pooling operations, processing deep patterns using contraction and expansion routes.

Using the transposed convolutions, the expansion path gradually restores the dimension of the activations while attempting to maintain the learned characteristics [14]. The tumor segmenter component classifies tumor areas into 'WT' (Whole Tumor), 'TC' (Tumor Core), and 'ET' (Enhancing Tumor) by combining features from the tumor extractor using upsampling. With the exception of the final output layer, which uses sigmoid activation for voxel classification, the model uses Leaky Rectified Linear Unit (LReLU) activation for convolution operations.

3.1 Data pre-processing

Due to unequal intensity distributions, intensity inhomogeneity in MRI multi-modality scans produces a bias field issue that degrades image quality and makes analysis more difficult, especially for segmentation tasks.

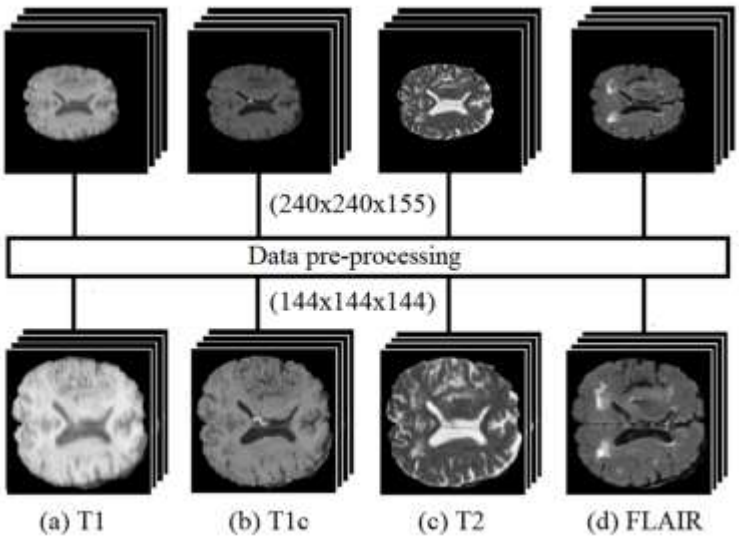

Figure2. Data pre-processing

Furthermore, the dark voxels representing background regions are removed for each modality and resized to 144×144×144 as shown in Figure. 2.

3.2 Tumor segmentation

Using 1x1 convolution with three filters and spatial dropout, the tumor segmenter analyzes feature maps from the RI-32, RI-16, RI-8, and RI-3 layers to produce a 3×h×w×d volume that corresponds to the "WT," "TC," and "ET" tumor regions. In order to make the complex volumes compatible with addition operations with upper layers along the batch axis, they are upsampled to match the sizes of the above layers. This convergence occurs at 3×144×144×144. In order to calculate the segmentation loss for the expected "WT," "TC," and "ET" areas, the final activation maps voxel intensities to the range [0,1] using a sigmoid function.

3.3 Inception module

It is difficult to identify things with different sizes and forms, such as brain tumors, using a single type of convolution because of their varied features; multi-scale or adaptive techniques are frequently more successful. The design of the framework's first module architecture. Concatenated 1×1, 3×3, and 5×5 kernel convolutions make up the initial block, which is followed by a 1×1 convolution to determine the relationships between multi-scale feature representations. To improve feature extraction and representation, instance normalization, LReLU activation, and 3D max pooling with downsampling come before each convolution. All of the suggested components are built using this module as its foundation.

IV RESULT AND DISCUSSION

A comprehensive dataset for nuclei recognition and segmentation tasks, the Kaggle Data Science Bowl 2018 dataset is made up of nuclei images with RGB channels that are separated into two stages: Stage 1 includes 670 training/validation photos and 65 test images, while Stage 2 has 3019 test images. A variety of situations are represented in these photos, including variations in cell type, magnification, and modality (brightfield/fluorescence). For model training and testing, each nucleus in the Stage 1 training set has annotated ground truth masks that are scaled to 128×128×3. For every full image, a comprehensive ground truth mask is created by combining the individual mask images. The ground truth masks for the test sets in stages 1 and 2 could not be used for experiments because they are not publicly available. In order to train and test the IU-Net model, the labeled data samples from stage 1 are split into 70% training data and 30% testing or validation data.

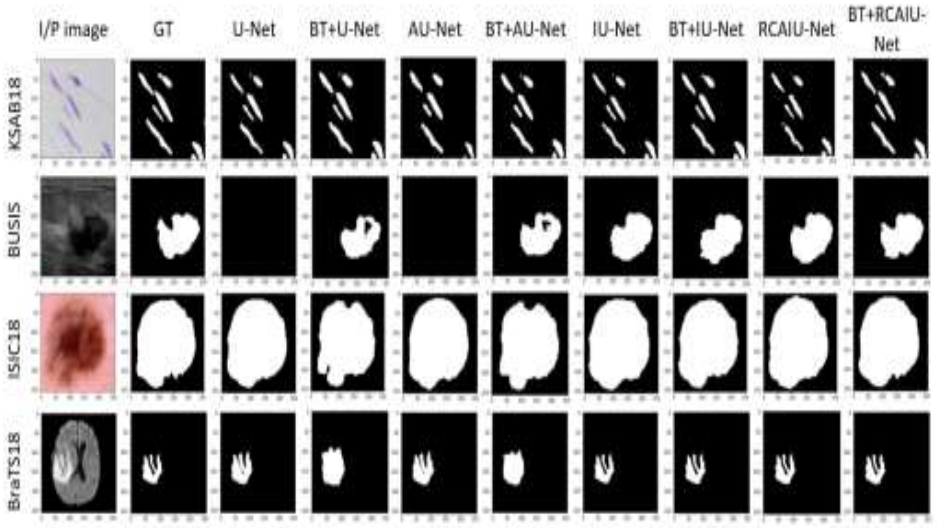

Figure 3. Comparison of segmentation results

The classification scores for each categorical label are included in the semantic segmentation that is returned for testing on the input image. The evaluation method is demonstrated in Figure 3 by superimposing the segmented images that are the result. True positive pixels tumor pixels that have been correctly classified are white in color. The results are perfect in terms of tumour detection, but the tumour appears larger than it actually is, as can be seen from this figure. In contrast, the results of case 1 are the least accurate.

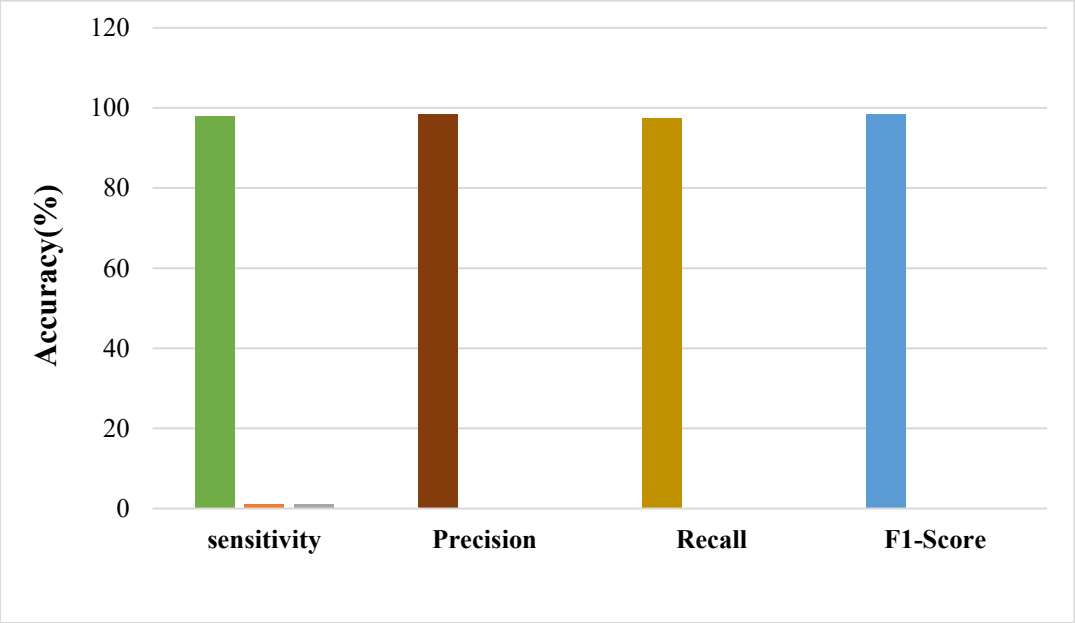

Figure 4: Performance metrics

The background tissue's size is significantly smaller than the tissue that needs to be segmented. The segmentation performance is greatly impacted by this. For instance, Figure 4 ratio of white to black pixels demonstrates a significant difference. With 99.6% accuracy, 97.89% sensitivity, 97.5% recall, 98.6% F1-Score, and 98.44% precision, the suggested classifier achieved the best performance, as shown in Figure 4.

CONCLUSION

The Modified U-Net for liver and tumor segmentation using deep learning is presented in this article. It outperforms existing models with high DSC values of 96.15% for liver and 89.38% for tumor segmentation on the LITS dataset (256×256) and 69.80% for tumor segmentation on the 3Dircadb

dataset (128×128). In the future, several CNN models can be evaluated to identify the smallest tumors, and real-time photos of hospitals of various sizes can be used to train and evaluate the model's effectiveness. In addition to DSC, volumetric analysis of the medical pictures and other factors can be used to evaluate the segmentation. Lastly, the datasets of various organs can also be segmented automatically.

REFERENCES

1. Vázquez-Lema, David, Eduardo Mosqueira-Rey, Elena Hernández-Pereira, Carlos Fernandez-Lozano, Fernando Seara-Romera, and Jorge Pombo-Otero. "Segmentation, classification and interpretation of breast cancer medical images using human-in-the-loop machine learning." *Neural Computing and Applications* 37, no. 5 (2025): 3023-3045.
2. Banjac, S., Papuga, S., & Broćeta, G. (2025). Sustainable Construction and The Use of Prefabricated Concrete. *Archives for Technical Sciences, 1(32),* 1–14. https://doi.org/10.70102/afts.2025.1732.001
3. Jayapradha, J., Su-Cheng Haw, Naveen Palanichamy, Senthil Kumar Thillaigovindhan, and Mutaz Al-Tarawneh. "Lung tumor segmentation in medical imaging using U-NET." *Journal of Informatics and Web Engineering* 4, no. 1 (2025): 140-151.
4. Rahman, M. A., Pramanik, M. M. H., Hasan, M. M., Ahmed, T., Alam, M. A., Hasan, S. J., ... & Mahmud, Y. (2024). Sixth sanctuary identification research and establishment strategy for enhancing production and conservation management of Hilsa (Tenualosa ilisha) in Bangladesh. *International Journal of Aquatic Research and Environmental Studies*, *4*(1), 37-47. https://doi.org/10.70102/IJARES/V4I1/4
5. Manjunath, R.; Kwadiki, K. Automatic liver and tumour segmentation from CT images using Deep learning algorithm. Results Control Optim. 2022, 6, 100087.
6. Aravindhan, S. (2023). A Flexible Structure's Active Vibration Suppression Using Smart Materials. *Association Journal of Interdisciplinary Technics in Engineering Mechanics*, *1*(1), 55-61.
7. Karthik, R.; Radhakrishnan, M.; Rajalakshmi, R.; Raymann, J. Delineation of ischemic lesion from brain MRI using attention gated fully convolutional network. Biomed. Eng. Lett. 2021, 11, 3–13.
8. Hasan, M. S. (2024). The Application of Next-generation Sequencing in Pharmacogenomics Research. *Clinical Journal for Medicine, Health and Pharmacy*, *2*(1), 9-18.
9. Birjais, Roshan. "Challenges and Future Directions for Segmentation of Medical Images Using Deep Learning Models." *Deep Learning Applications in Medical Image Segmentation: Overview, Approaches, and Challenges* (2025): 243-264.
10. Shimazu, S. (2023). Maximizing Employee Satisfaction Through Wellness Initiatives. *Global Perspectives in Management*, *1*(1), 49-65.
11. Amin, J.; Anjum, M.A.; Sharif, M.; Kadry, S.; Nadeem, A.; Ahmad, S.F. Liver Tumor Localization Based on YOLOv3 and 3D-Semantic Segmentation Using Deep Neural Networks. Diagnostics 2022, 12, 823.
12. Reddy, S., & Verma, M. (2024). Enhancing Patient Comprehension through Simplified Medical Terminology: A Literacy-based Approach. *Global Journal of Medical Terminology Research and Informatics*, *2*(1), 1-3.
13. Karthik, R.; Radhakrishnan, M.; Rajalakshmi, R.; Raymann, J. Delineation of ischemic lesion from brain MRI using attention gated fully convolutional network. Biomed. Eng. Lett. 2021, 11, 3–13.
14. Karthik, V. P., Rajadurai, V., Nandhalkumar, V., Rajakumaran, M., & Prakash, R. (2018). Design and Fabrication of Artificial Draught System in Welding Booth. *International Journal of Advances in Engineering and Emerging Technology*, *9*(1), 1–3.
15. Ayalew, Y.A.; Fante, K.A.; Mohammed, M.A. Modified U-Net for liver cancer segmentation from computed tomography images with a new class balancing method. BMC Biomed. Eng. **2021**, 3, 4